Numerical Upscaling of Electrical Conductivity: A problem specific approach to generate coarse-scale models

L. A. Caudillo-Mata, E. Haber, L. J. Heagy and D. W. Oldenburg*
Geophysical Inversion Facility, Earth, Ocean and Atmospheric Sciences Department, University of British Columbia
2207 Main Mall, V6T 1Z4 Vancouver, British Columbia, Canada

SUMMARY

In this work we propose a new approach for the upscaling problem of electrical conductivity in the context of electromagnetic methods. We pose the upscaling problem as a parameter estimation problem, which allow us to develop a goal-oriented, quantitative framework that combines widely used simulation tools such as Mimetic Finite Volume, inversion and optimization techniques. We thus create a flexible methodology that allows the users to estimate, in an affordable manner, coarse-scale conductivity models that approximate, in some sense, the fine-scale ones. Our framework is based on the observation that for any conductivity model a number of different criteria can be considered for the homogenization problem. In particular, different physical fields and fluxes can be considered. Our framework allows the choice of the criteria that is the most appropriate for the goal of the simulation. Results are illustrated with a couple of simulations that demonstrate the capabilities of our method as well as the challenges that this different perspective offers.

INTRODUCTION

Electromagnetic (EM) methods have a variety of applications in resource exploration, particularly, in mining and oil and gas. The behavior of an EM field is controlled by three primary properties of the medium, the electrical conductivity, Σ, the dielectric permittivity, ε, and the magnetic susceptibility, μ, as well as the location of the sources and the frequencies. For a given source, and within the frequency range typical of most EM geophysical surveys, variations in electrical conductivity are generally the main controlling factor in the response of the EM fields (Ward and Hohmann, 1988; Oldenburg and Pratt, 2007; Zhdanov, 2010). As such, EM methods are powerful tools for characterizing the electrical conductivity of a geologic setting.

Numerical modeling and inversion techniques provide a means of understanding the connection between the EM responses observed and the underlying electrical conductivity structures (e.g. Oldenburg and Pratt (2007)). Finite Volume and Finite Element methods, as well as integral equations, have been studied extensively and applied in many geophysical applications of EM. However, these methods are limited in their ability to accurately simulate realistic situations. True geologic settings are heterogeneous over a range of length scales and their physical properties may vary over orders of magnitude, from millimeters to hundreds of meters, requiring very fine meshes. Such meshes are difficult, if not impossible, to work with and lead to simulations which are extremely expensive to compute Durlofsky (2003).

Numerical upscaling is a computational procedure that strives to develop coarse scale models that accurately approximate fine scale ones. These models attempt to capture the physical response due to the fine-scale heterogeneities while reducing the size of the problem thus, alleviating the computational cost.

In this paper, we adopt and extend the numerical upscaling techniques developed in the context of flow in porous media (Durlofsky, 1998, 2003; Gerritsen and Durlofsky, 2005) to EM. We propose a framework, within the context of parameter estimation problems, to upscale the electrical conductivity for a heterogeneous medium using the Quasi-Static Maxwell's Equations in Frequency Domain. We do this by selecting a physical response on the fine scale which we aim to reproduce on the coarse scale. As we show, the solution to the parameter estimation problem is highly dependent on, and specific to, the choice in boundary conditions and the upscaling criteria chosen. These factors determine how the system is excited and which physical response we measure. This feature allows for physical behaviors of interest on the fine scale to be preserved on a coarse scale.

MATHEMATICAL MODELING

Finite Volume Discretization of Maxwell's Equations

Let Ω be a finite three-dimensional cuboid region with boundary $\partial\Omega$. We consider the quasi-static, first order form of Maxwell's equations in the frequency domain with non-homogeneous Dirichlet boundary conditions

$$\nabla \times \vec{E} + i\omega\vec{B} = \vec{0}, \qquad \forall x \in \Omega, \tag{1}$$

$$\nabla \times \mu^{-1}\vec{B} - \Sigma\vec{E} = \vec{s}, \qquad \forall x \in \Omega, \tag{2}$$

$$(\nabla \times \vec{E}) \times \vec{n} = \vec{E}_0, \qquad \forall x \in \partial\Omega, \tag{3}$$

where $\vec{E}$ is the electric field, $\vec{B}$ is the magnetic flux density, $\vec{s}$ is the source term, ω is the angular frequency and $\vec{n}$ is the unitary outward-pointing normal vector. The material parameters, μ and Σ, are the magnetic permeability and electrical conductivity, respectively. In general, both the permeability and conductivity are given by 3×3 symmetric positive definite (SPD) tensors.

We apply the Mimetic Finite Volume method (MFV) to discretize the weak form of the system (1)-(3). MFV is an extension of Yee's method that allows for highly heterogeneous and anisotropic media to be discretized in a conservative manner, leading to symmetric linear systems (Yee, 1966; Hyman and Shashkov, 1999a,b). We use a Yee grid (staggered 3D tensor mesh) and discretize $\vec{E}$ on the edges, $\vec{B}$ on the faces and the material properties μ and Σ at the cell-centers of the mesh. Hence, we obtain the second order discretization for our system given by

$$\mathbf{A}(\boldsymbol{\Sigma})\mathbf{e} = -i\omega(\mathbf{q} + \mathbf{q}_{bc}) \tag{4}$$

with

$$\mathbf{A}(\boldsymbol{\Sigma}) = \mathsf{CURL}^\top \mathbf{M}_f(\boldsymbol{\mu}^{-1})\mathsf{CURL} + i\omega \mathbf{M}_e(\boldsymbol{\Sigma}), \quad (5)$$

$$\mathbf{q}_{bc} = \mathsf{CURL}^\top \mathbf{M}_f(\boldsymbol{\mu}^{-1})\mathbf{P}\big|_{\partial\Omega}, \quad (6)$$

where $\boldsymbol{\Sigma}$, $\boldsymbol{\mu}$, $\mathbf{e}$, $\mathbf{q}$ and $\mathbf{q}_{bc}$ represent the discrete approximation at the corresponding mesh points for Σ, μ, $\vec{E}$, $\vec{s}$, and the boundary conditions (3), respectively. Additionally, CURL, $\mathbf{M}_f(\boldsymbol{\mu}^{-1})$ and $\mathbf{M}_e(\boldsymbol{\Sigma})$ are the corresponding discrete operators for the continuous operator $\nabla\times$ and the mass matrices for the material properties μ and Σ. Finally, $\mathbf{P}$ is the matrix that takes the boundary conditions and prolongs the vector to the right dimensions and signs.

From (4), we observe that the discrete electric field $\mathbf{e}$ can be expressed as $\mathbf{e}(\boldsymbol{\Sigma})$, that is, we must solve a forward problem in order to compute $\mathbf{e}$. This system of equations can be solved using direct or iterative methods, see Haber and Ascher (2001).

Numerical Upscaling Method

Our numerical approach poses upscaling as a parameter estimation problem. Given a mathematical model which has been discretized on a fine mesh, we aim to find a model of the *upscaled conductivity* which varies on a coarse mesh and is equivalent, in some sense, to the fine scale model. We formulate the search for the upscaled model as an optimization problem in terms of the upscaled conductivity. One of the main advantages of this approach is that it is general enough to deal with a broad variety of fine scale conductivity structures.

We consider a very large, finely discretized 3D tensor mesh and some nested partition of a coarser mesh. Let Ω' be a coarse-mesh cell. In addition, let Ω_h and Ω_H be the discretization of Ω'. Consider the upscaling problem for a single coarse-mesh cell, Ω', which is composed of many fine mesh cells with heterogeneous conductivity, see Figure 1. Such a coarse-mesh cell resides within our large mesh.

We denote the discrete fine mesh conductivity and the discrete upscaled coarse mesh conductivity as $\boldsymbol{\Sigma}_h$ and $\boldsymbol{\Sigma}_H$, respectively. In addition, let $(\mathbf{e}_h, \mathbf{b}_h, \mathbf{j}_h)$ and $(\mathbf{e}_H, \mathbf{b}_H, \mathbf{j}_H)$ be the discrete approximations to the electric fields, magnetic fluxes and electric current densities in Ω' that correspond to the fine and upscaled conductivities, respectively.

The **goal of our method** is to construct an upscaled electrical conductivity, $\boldsymbol{\Sigma}_H$, for each coarse-mesh cell Ω' such that the corresponding downscaled physical responses $(\mathbf{e}_H, \mathbf{b}_H, \mathbf{j}_H)$ accurately approximate the fields and fluxes $(\mathbf{e}_h, \mathbf{b}_h, \mathbf{j}_h)$ generated by the fine model conductivity, $\boldsymbol{\Sigma}_h$. The upscaled quantity, $\boldsymbol{\Sigma}_H$, must be able to capture some of the existing heterogeneity in $\boldsymbol{\Sigma}_h$, as well as having a smaller number of parameters compared to $\boldsymbol{\Sigma}_h$. Thus, for the coarse-mesh cell Ω', discretized into n^3 fine mesh cells of size h^3, we parametrize $\boldsymbol{\Sigma}_H$ as a SPD tensor, composed of only 6 real values,

$$\boldsymbol{\Sigma}_H(\sigma_1,\sigma_2,\sigma_3,\sigma_4,\sigma_5,\sigma_6) = \begin{bmatrix} \sigma_1 & \sigma_4 & \sigma_5 \\ \sigma_4 & \sigma_2 & \sigma_6 \\ \sigma_5 & \sigma_6 & \sigma_3 \end{bmatrix}. \quad (7)$$

In order to upscale the variable conductivity $\boldsymbol{\Sigma}_h$ into $\boldsymbol{\Sigma}_H$, we envision a number of possible experiments where boundary conditions on the electric or magnetic fields around Ω' induce a physical response. We do not include a source term in the model, although this can be easily added if needed. The choice of boundary conditions as well as the physical response we intend to simulate, influence how the fields and fluxes sample the fine-scale conductivity structure and how they should be upscaled. Hence the selection of an appropriate set of boundary conditions and physical responses is crucial.

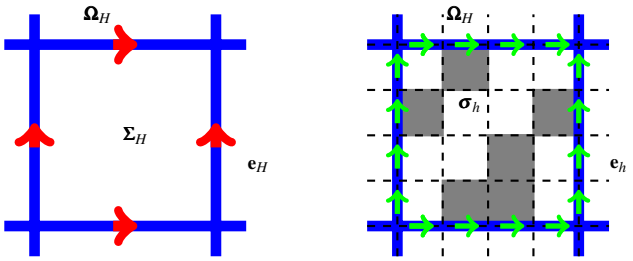

Figure 1: Left: 2D view of the coarse-mesh cell Ω_H. The discrete coarse electric fields $\mathbf{e}_H$ are allocated on the edges, and the coarse electric conductivity $\boldsymbol{\Sigma}_H$ is located at the cell-center. Right: 2D view of a coarse-scale cell Ω_H composed of fine scale mesh cells (dashed black line) with heterogeneous conductivity, $\boldsymbol{\sigma}_h$, and the discrete fine electric fields ($\mathbf{e}_h$) on the edges at the boundary of Ω_H.

Here, we impose a set of $N = 12$ boundary conditions on the modeling domain. This allows us to solve for the discrete electric fields *locally inside* Ω' using (4), while taking into consideration the structure of the fine-scale electrical conductivity. Each boundary condition takes the value 1 on a given edge, and decays linearly to 0 in the other two directions, see Figure 2. This set of boundary conditions samples the fine-scale conductivity structure from multiple directions, allowing us to observe coarse-scale anisotropy. Our model can easily be extended to consider more general boundary conditions (see discussion in the summary).

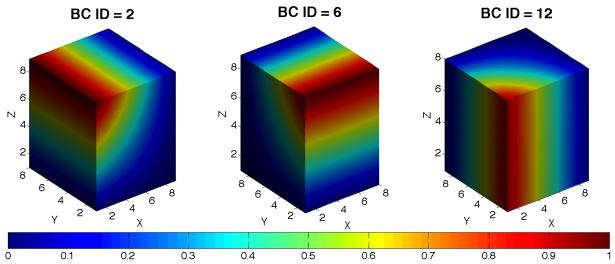

Figure 2: Example of three out of the twelve boundary conditions imposed to locally interpolate and sample the electric fields inside Ω'.

Given the boundary conditions, we define the *best* upscaled conductivity on Ω' as

$$\boldsymbol{\Sigma}_H^* = \underset{\boldsymbol{\Sigma}_H \in \mathscr{S}_3^+}{\arg\min} \quad \phi(\boldsymbol{\Sigma}_H) = \frac{1}{2}\sum_{k=1}^{N} \left\| f_k^{\text{pred}}(\boldsymbol{\Sigma}_H) - f_k^{\text{obs}} \right\|_2^2, \quad (8)$$

$$\text{subject to} \qquad \boldsymbol{\Sigma}_H \succ \mathbf{0},$$

where $\mathscr{S}_3^+$ is the set of 3×3 SPD matrices, $\mathbf{\Sigma}_H$ is given by (7) and N is the number of boundary conditions (i.e. the number of ways we excite the system (4)). The physical response is captured by the function f, which is evaluated at the points of comparison using a projection of the discrete electric or magnetic fields or fluxes. For example, the total current flux or magnetic flux density though a particular face of Ω'. In particular, f^{obs} is the physical response due to the true fine scale conductivity structure, $\mathbf{\Sigma}_h$, and $f_k^{\text{pred}}(\mathbf{\Sigma}_H)$ is that due to the upscaled conductivity structure, $\mathbf{\Sigma}_H$. These quantities are computed by solving N forward problems of the form (4). This optimization problem can be solved using the projected Gauss-Newton method (Kelley, 1999; Lin and Moré, 1999; Nocedal and Wright, 2006).

We refer to the function $\phi(\mathbf{\Sigma}_H)$ as the *upscaling criterion*. It is a ruler that assesses the quality of a particular $\mathbf{\Sigma}_H$. We want to emphasize that the formulation given in (8) provides a large variety of upscaling criterion options. Consequently, the results will strongly depend upon the choices made in the definition of $\phi(\mathbf{\Sigma}_H)$.

SYNTHETIC EXAMPLES

To demonstrate the upscaling procedure and the impact of the choice in upscaling criterion, we consider two synthetic examples, as shown in Figure 3: the canonical model of an isolated block (a), and that of a sheet (b). In both cases, we consider the upscaling domain (Ω') to be given by a cuboid region with dimensions $100m\times 100m\times 100m$. We extend the forward modeling domain a further $50m$ in each direction such that Ω' is positioned in the center. We discretize the entire domain using uniform fine mesh cells which are $12.5m\times 12.5m\times 12.5m$. Hence the total number of fine cells is 16^3 and Ω' includes 8^3 fine cells. We assume the fine scale conductivity model, $\mathbf{\Sigma}_h$, to be isotropic, and allow the upscaled conductivity model, $\mathbf{\Sigma}_H$, to be parametrized by 6 values as in (7). The magnetic permeability is taken to be that of free space, namely $\mu = 4\pi\times 10^{-7}$.

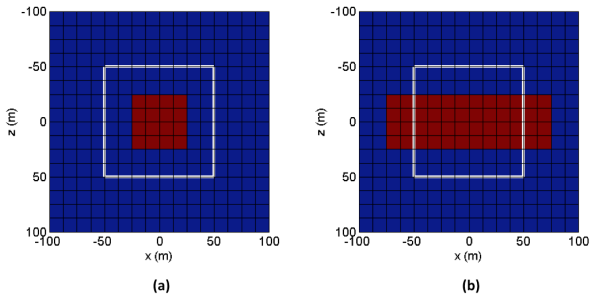

Figure 3: Cross sections of the fine scale conductivity model for (a) the isolated block and (b) the sheet. Conductive bodies are displayed in red. The resistive background is displayed in blue. The coarse-mesh cell, Ω', which we aim to upscale is outlined in white.

For the upscaling, we must select a criterion by which we judge the quality of the upscaled conductivity, $\mathbf{\Sigma}_H$. For the following examples, we consider two criteria on Ω': 1) $\mathbf{j}-$criterion: the total current density flux on each of the six faces of Ω', and 2) $\mathbf{b}-$criterion: the total magnetic flux on each of the six faces of Ω'. The total flux (either current density or magnetic field) over each face is evaluated by computing the surface integral of the flux through that face.

E1: Conductive block in a resistive background

First, we study the case of a conductive block in a resistive background. Assume that inside Ω' there is a $50m\times 50m\times 50m$ conductive block, located at its center, as shown in Figure 3 (a). The surrounding material is resistive ($10^{-4}\ S/m$). For this example, we use a frequency of $1Hz$ and consider three different conductivities of the block, 10^{-2}, 10^{-1} and $1\ S/m$.

We applied the **b** and **j** upscaling criteria described above, and obtained the upscaled conductivity values shown in Figure 4. Note that we recovered an isotropic (scalar-valued) $\mathbf{\Sigma}_H^*$ in each scenario, as expected due to the symmetry of the model.

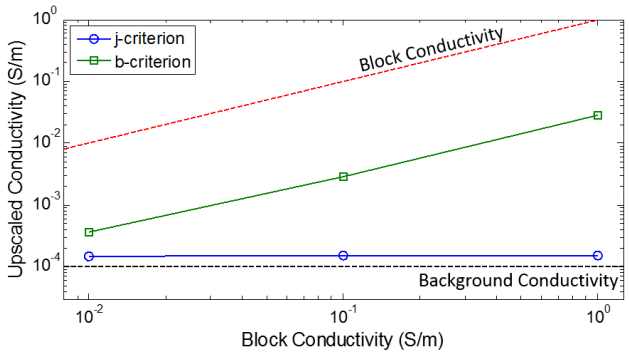

Figure 4: Upscaled conductivity results found using the **j** and **b** criteria for the block model shown in Figure 3 (a). Note that the upscaled conductivity in this case can be defined by a scalar, as the tensor recovered was diagonal, with all diagonal elements being equal.

Clearly, there is a large discrepancy between the upscaled conductivities recovered using the **b** and **j** upscaling criteria for each of the three block conductivities. Physically, this discrepancy can be reconciled by recognizing that the current density $\vec{J}$, and magnetic flux density $\vec{B}$ reflect different physical processes. Current is the flow of charges through a material. In the case of a conductive block in a resistive background, the current must be driven through the resistive background irrespective of the conductivity of the block. Thus, the resistive background dominates the upscaled conductivity recovered using the **j**-criterion. On the other hand, magnetic flux is produced as a result of induced currents. Currents can be induced in the conductive block regardless of the conductivity of the background. Therefore, we see that the conductivity of the block dominates the upscaled conductivity recovered using the **b**-criterion.

E2: Conductive sheet in a resistive background

Next, we examine the case of a conductive sheet in a resistive background ($10^{-4}\ S/m$) positioned at the center of Ω', as shown in Figure 3 (b). It has dimensions $150m\times 150m\times 50m$.

Note that the sheet is extended outside of the cell we are upscaling, Ω', in order to reduce the impact of edge effects. It is stopped short of the boundary of the modeling domain in order to avoid applying the boundary conditions directly on the sheet. For this simulation, we use a frequency of $1Hz$.

Now that the model is no longer identical in each direction, we expect to recover an anisotropic upscaled conductivity. In particular, we expect a diagonal tensor, where $\sigma_1^* = \sigma_2^*$ which is distinct from σ_3^*.

Typically, one would draw the analogy between layered conductors and a simple circuit model. In this case, we would expect that the components of the upscaled conductivity tensor, σ_1^* and σ_2^* would conform closely the approximation of conductors in parallel, while σ_3^* would be similar to the approximation of conductors in series. Note however, that this approximation accounts for only one physical behavior, galvanic current flow, to which the **j**-criterion is sensitive. It does not account for any inductive currents, to which the **b**-criterion is sensitive.

To investigate, we again assign the electrical conductivity of the background to be $10^{-4}S/m$ and examine three conductivities for the sheet, $10^{-2}S/m$, $10^{-1}S/m$ and $1S/m$. Using both the **b** and **j** criteria, we perform the upscaling, and recover the upscaled conductivities shown in Figure 5.

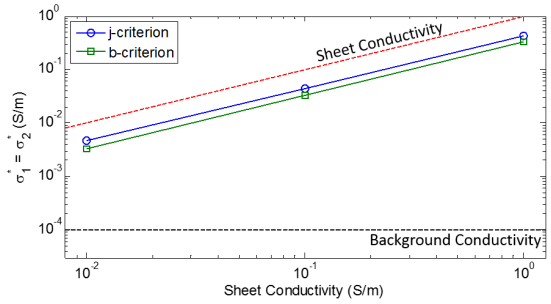

(a)

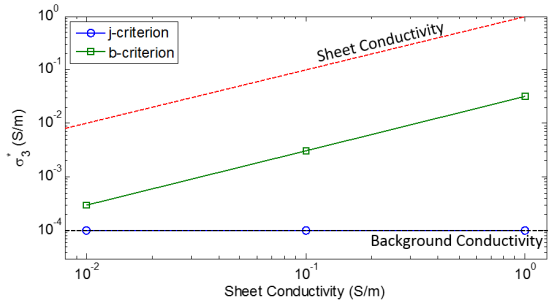

(b)

Figure 5: Upscaled conductivity results found using the **j** and **b** criteria for the sheet model shown in Figure 3 (b). Note that the upscaled conductivity tensor can be described by two values, as it is a diagonal tensor and $\sigma_1^* = \sigma_2^*$. $\sigma_1^* = \sigma_2^*$ is shown in plot (a), and σ_3^* is shown in plot (b).

In this case, the recovered upscaled conductivity $\boldsymbol{\Sigma}_H^*$ is a diagonal tensor with two unique components: $\sigma_1^* = \sigma_2^*$ and σ_3^*, see equation (7). Figure 5 (a) shows the σ_1^*, σ_2^* components of the tensor and Figure 5 (b) shows the σ_3^* component. The values recovered using the **j**-criterion conform well to the parallel and series circuit approximations for $\sigma_1^* = \sigma_2^*$, and σ_3^*, respectively. For each scenario the σ_3^* recovered using the **j**-criterion is nearly identical to the resistive background, as is to be expected using a series circuit approximation. Similar to the block model results, this is as a consequence of having to drive the current through the resistive background in the z-direction, regardless of the conductivity of the sheet. However, for the σ_1^*, σ_2^*, the conductivity of the sheet has a large impact on the value we recover. In this case, the conductive sheet forms a connected pathway from one side of the cell we aim to upscale to the other along both horizontal directions. As a result, current is channeled along this pathway, causing the conductivity of the sheet to have a large impact on the σ_1^*, σ_2^* components of the upscaled conductivity, as shown in Figure 5.

Using the **b**-criterion, we see that the conductivity of the sheet has a significant impact on both the $\sigma_1^* = \sigma_2^*$ (Figure 5 (a)) components and the σ_3^* component (Figure 5 (b)), contrary to the parallel-series circuit approximations. This is again because the magnetic flux density is sensitive to inductive currents. Since the sheet has a finite thickness, these currents can be induced in any direction, and therefore contribute to the upscaled values σ_1^*,σ_2^* and σ_3^* we recover using the **b**-criterion.

CONCLUSIONS

The upscaled conductivity model is specific to, and highly dependent on, the experiment posed. As a result, it allows for physical behaviors of interest on the fine scale to be preserved on a coarse scale.

As discussed in the block and sheet examples, the current density and magnetic flux density each sample the conductivity structure differently, and are therefore sensitive to different features of the model. As a result, the recovered upscaled conductivities using either method may vary over orders of magnitude. Therefore, for a given fine scale conductivity structure, there is no a unique upscaled model which completely describes it.

Through the simulations we have performed, we have demonstrated the significance of choice of boundary conditions and upscaling criterion on the resulting upscaled conductivity. This is a reflection of the fact that an upscaled quantity is a property we construct, and it will take on different values, depending on how we formulate the problem. This is a powerful idea, and can be used to tackle problems with a different perspective when care is taken to properly define the question being asked.

ACKNOWLEDGMENTS

The authors would like to thank Christoph Schwarzbach and Ives Macedo for the discussions held regarding the Mathematical Modeling section.

REFERENCES

Durlofsky, L. J., 1998, Coarse scale models of two phase flow in heterogeneous reservoirs: volume averaged equations and their relationship to existing upscaling techniques: Computational Geosciences, **2**, 73–92.

———, 2003, Upscaling of geocellular models for reservoir flow simulation: a review of recent progress: 7th International Forum on Reservoir Simulation Bühl/Baden-Baden, Germany, 1–58.

Gerritsen, M. G., and L. J. Durlofsky, 2005, Modeling fluid flow in oil reservoirs: Annual Review of Fluid Mechanics, **37**, 211–238.

Haber, E., and U. Ascher, 2001, Fast finite volume simulation of 3D electromagnetic problems with highly discontinuous coefficients: SIAM Journal on Scientific Computing, **22**, 1943–1961.

Hyman, J., and M. Shashkov, 1999a, Mimetic discretizations for Maxwell's equations: Journal of Computational Physics, **151**, 881–909.

———, 1999b, The orthogonal decomposition theorems for mimetic finite difference methods: SIAM Journal on Numerical Analysis, **36**, 788–818.

Kelley, C., 1999, Iterative methods for optimization.

Lin, C., and J. Moré, 1999, Newton's method for large bound-constrained optimization problems: SIAM Journal on Optimization, **9**, 1100–1127.

Nocedal, J., and S. J. Wright, 2006, Numerical Optimization, 2nd ed.: Springer New York.

Oldenburg, D. W., and D. A. Pratt, 2007, Geophysical inversion for mineral exploration: A decade of progress in theory and practice: Proceedings of exploration.

Ward, S., and G. Hohmann, 1988, Electromagnetic theory for geophysical applications, *in* Electromagnetic methods in applied geophysics: Society of Exploration Geophysicists, **1**, 4, 130–311.

Yee, K., 1966, Numerical Solution of Initial Boundary Value Problems Involving Maxwells Equations in Isotropic Media: Antennas and Propagation, IEEE Transactions on, **14**, 302–307.

Zhdanov, M., 2010, Electromagnetic geophysics: Notes from the past and the road ahead: Geophysics, **75**, 75A49–75A66.